Structural and Aerodynamics Analysis on Different Architectures for the Elettra Twin Flyer Prototype

09ATC-0382

Structural and Aerodynamics Analysis on Different Architectures for the Elettra Twin Flyer Prototype

P. Gili, M. Battipede, M. Vazzola
Aeronautical and Space Department, Politecnico di Torino – 10129 Torino, ITALY

M. Visone, P.Farina
Blue Engineering, ITALY

ABSTRACT

This paper deals with the design and development of an innovative airship concept which is remotely-controlled and intended to be used for monitoring, surveillance, exploration and reconnaissance missions. Two potential solutions have been analyzed: the first consists of a *double-hull* configuration, characterized by the presence of a primary support structure connected by appropriated bindings to a couple of twin inflatable hulls. The second architecture is a *soap-shaped* exoskeleton configuration which features a single inflated section, incorporating two separate elements held internally by a system of ribs. The aim of this study is to analyze and compare the two configurations, to determine the most appropriate solution in terms of performance, cost and maneuvering capabilities

INTRODUCTION

The low-cost multi-purpose multi-mission platform Elettra-Twin-Flyers (ETF) is being developed by the synergy of BLUE Engineering, Nautilus S.p.A and the Politecnico di Torino[1]. It is a very innovative remotely-controlled airship equipped with high precision sensors and telecommunication devices. For its peculiar features, it is particularly suitable for inland, border and maritime surveillance missions and for telecommunication coverage extensions, especially in those areas which are either inaccessible or without conventional airport facilities and where the environmental impact is an essential concern.

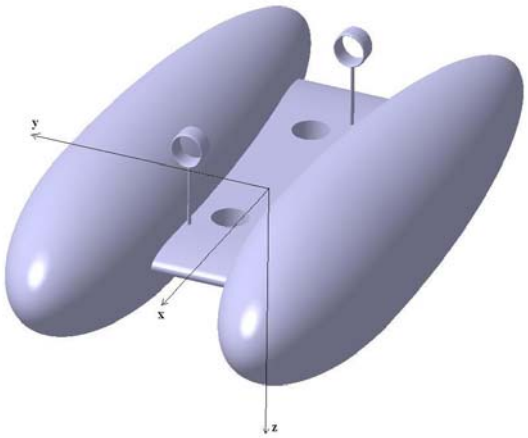

Figure 1 – Elettra Twin Flyers demonstrator.

ETF is characterized by great maneuverability as well as low wind sensitivity[2]. Flight conditions range from forward, backward and sideward flight to hovering, both in normal and severe wind conditions. To achieve these capabilities the ETF has been conceived with a highly non conventional architecture. The key point of the design is the innovative command system, which is completely based on thrust-vectoring propellers moved by electrical motors, powered by hydrogen fuel cells.
Flight tests are in progress on a flight demonstrator[3], which is a reduced-scale reduced-complexity platform, purposely assembled to test the most critical subsystems, such as the command system and the architectural solution. The demonstrator architecture is shown in Figure 1.

With appropriate axis rotation and variation of the rotational speed of the six propellers, this configuration enables control in 6 Degrees-of-Freedom (DOF). The command system does not need to have a relative speed to be effective, and this means that this airship has real hovering capabilities. Moreover, this command system has been conceived to be oriented in the wind direction, so that this airship can point its payload towards a given target whatever the wind direction is, both in hovering and forward flight.
During hovering, altitude is maintained by the synergy of the helium buoyancy and the vertical propellers' thrust. Forward movement creates an additional aerodynamic lift which is generated as a result of the air-flow circulation over the hulls. The complete absence of aerodynamic control surfaces not only increases manoeuvrability at low speed, but eliminates a source of disturbance during operation in adverse weather conditions. An obvious consequence of this approach is that an higher power consumption is required to manoeuvre and, as power is limited and must be shared between propulsion and manoeuvre, a manoeuvrability capability reduction is clearly experienced at high speed. For the range of application for which this airship has been conceived, however, these drawbacks have been considered perfectly acceptable.

NEW AIRSHIP CONFIGURATIONS

Ground and flight tests are revealing that the architecture can be further optimized. For this reason the whole configuration is being reconsidered. Different architectures have been proposed and they are now being analyzed under manifold points of view. The criteria used during this phase will be highlighted in the next paragraph.

Generally speaking, the new configurations are evolutions of previous designs whereas the control system strategy is conceived in the same identical way, notwithstanding the number of propellers. They can be 8 or 10, 2 or 4 of which are fixed whereas 4 or 8 are manoeuvrable. As for the previous configuration, the new ETF06 does not have movable aerodynamic control surfaces.

Low environmental impact is guaranteed by the employment of electric motors as well as by the power system, based on hydrogen fuel cells and auxiliary batteries or supercapacitors which supply extra energy to cope with the peaks resulting from abrupt manoeuvres.
To make the aerodynamic and structural analyses cost-effective, two configurations has been selected as the most representative. The two alternative solutions are the following:

- The first is a direct derivation of the demonstrator – the *double-hull* solution (Figure 2). This is characterised by a main structure, connected to the two gas envelopes by means of a set of elongated S-shape clamps. Among the available aeronautical technologies, the aluminium truss and the carbon sandwich structures have been considered.

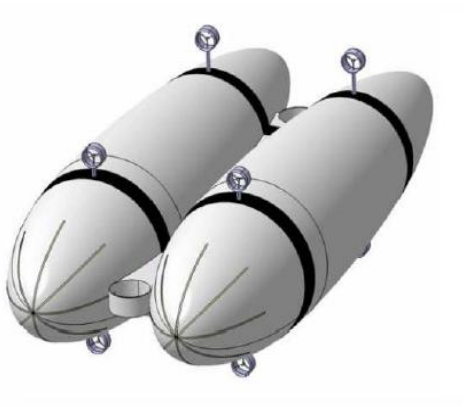

Figure 2 – Non-rigid double-hull configuration

- The second solution is distinctly different from the demonstrator, above all because it is a rigid structure – this is known as the *soap-shaped* or *exoskeleton* design (Figure 3). It features a single hull formed from the union of two parallel hulls, supported internally by a system of structural ribs. The structure of the *double-hull* is too complex to be realized by standard aluminium components, so only the carbon sandwich solution has been analyzed.

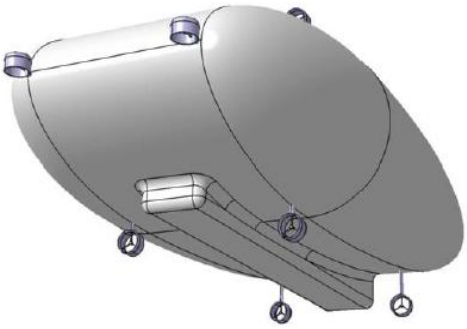

Figure 3 – Rigid soap-shaped configuration

COST FUNCTION DEFINITION

To select the best solution, a cost function is introduced to take into account a number of design criteria, which should bring to the configuration featuring the best ratio performance-over-cost. Each criterion is weighted according to its relative importance in the overall design. At the end of the process every configuration should be associated with an objective index which indicates the design excellence.
The following factors were considered:

- Overall dimension: the assumption is that the cost function varies linearly with the overall dimension; the associate cost weight is selected to give the parameter a medium-high importance;
- weight: evaluated as the overall dimension, but with a medium-low importance.

- wind sensitivity: as this is an aerodynamic consideration it is evaluated in terms of aerodynamic stability derivatives. The cost function has a quadratic relationship with the wind sensitivity which is weighted as to give the parameter high importance.
- handling and payload accommodation: since in both cases it is difficult to define a parameter that represents these criteria effectively, they are weighted as a constant cost and a medium importance is assigned.
- Acquisition and operating costs: the parameter is weighted linearly with a medium-high importance.
- Reliability, service life and maintenance (cost, mean time to repair, mean time to service…): these are parameters that can be considered similar if not equal for both solutions. As improvements of these parameters clearly implies increasing in the design and production costs, they have been considered linearly-increasing costs and a medium-high importance has been attributed to all of them.

Details of the structural analysis are contained in [4] and [5].

DOUBLE HULL CONFIGURATION

The double-hull configuration (Figure 2) is the classic design of two hulls separated by a central structure: The *nacelle* (the compartment in which the payload, power supply and avionics are located) is positioned beneath the line of contact between the two hulls, enabling television cameras, if installed, to be tilted and pointed downwards without any visual obstructions. Two large vertical propellers are positioned at the fore and aft ends of the central structure. Eight longitudinal–axis propellers are used for propulsion and orientation. They could be reduced to four which is the minimum number of effectors required for full maneuverability. The connecting structure is a central tube running in the longitudinal direction between the two S-shaped arms, which are rigid and are used to support the propellers (Figure 4).

This shaft is partitioned in five sections corresponding to the couple of S-shape forceps and three intermediate ribs, which support the nacelle

The hulls are secured to the structure through straps, which are fastened at all the five connection points. In this way the more critical loads, which are brought about by the buoyancy, can be uniformly distributed along the belt main resistant direction, whereas the aerodynamic forces are transmitted to the S-shaped structures. The same structures prevent the hulls form being pushed and eventually unhinged from their location. The aerodynamic drag, in fact, is contrasted by the belt friction and, more important, by the clasp action performed by the counteracting Ss which embrace the hulls on the two sides of the maximum diameter section.

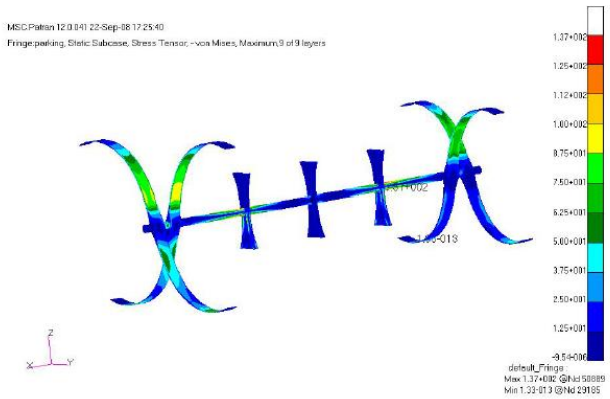

Figure 4 – Structure of the non-rigid double-hull configuration

The central shaft is the part to which all the other components are attached. Its length is proportional to the sum of the two semi-axes of the ellipses that constitute the hulls (around 0.6 times the total length); it must be sufficiently long to allow the supporting arms to encompass the hulls.

The supporting arms represent the most critical part of the design and due to their long and slender shape are likely to experience the most severe deflections. Excessive deformations must be carefully avoided to maintain the thrust forces in the nominal positions and minimize control discomforts. The central septa have mainly two functions: the first one concerns the hulls, as, together with the supporting arms, they help maintaining the envelopes rigidly connected to the structure. Its second function is to support the underneath nacelle.

In the model created for the simulation in MSC.NASTRAN, the nacelle was assumed to hang from the septa in the space between the two hulls and the connection was simulated with rigid elements. As with the supporting arms, the septa were intentionally designed to have three planes of symmetry.

The hulls' shape have been determined from aerodynamic consideration. It is very well known, in fact, that, for a single hull, the aerodynamic drag is strongly influenced by the slenderness ratio (length over radius). The slenderness ratio has then been selected as to minimize the drag in the whole speed envelope. For the same reason it has been decided to make the hull longitudinally non symmetrical, shaping the longitudinal section as two half-ellipses, one having its major axis equal to a third of the total length of the airship, the second having the major axis equal to the remaining two-thirds of the length. The minor axes are clearly coincident and equal to approximately one-eighth of the total length. The overall hull is then been designed as the revolution of the longitudinal section, whose dimensions have to be calculated iteratively as they affect two design parameters: the volume of helium that can be contained (and hence the aerostatic lift); and the surface area of the hulls, which is necessary to calculate the total mass.

SOAP-SHAPED (EXOSKELTON) CONFIGURATION

The second configuration is the exoskeleton (Figure 3), formed by drawing together and uniting the two hulls. The principal advantage is that for an equivalent length there is a volume increase of about 20%, which brings to extra helium volume and thus extra buoyancy. At least in theory, this leads to two possibilities: an the increasing in the payload capability or a decreasing of the structure length. What actually happen, however, is that the exoskeleton structure has a mass which is by far greater than the double-hull design of the same length.

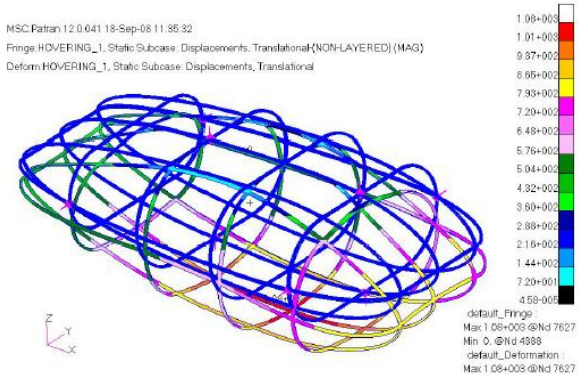

Figure 5 – Exoskeleton *of the soap-shaped configuration*

The structure of the exoskeleton is geodesic and is made up by eight "ribs" constituted by a T-section (Figure 5). There are four vertical propellers, positioned at the prow and the stern, and along the sides of the airship, in addition to the 8 (or 4 at least) thrust vectoring propellers positioned similarly to the double-hull configuration. For the exoskeleton there are more degrees of freedom for the propeller positioning , as they could be virtually attached to any longitudinal spar. Despite this, the number of propellers is reduced from eight to four – two positioned on top of the airship and two on the bottom side, all aligned with the longitudinal axis. The nacelle is still positioned underneath the hull, as for the double-hull configuration.
The envelope is no longer a single multilayer fabric: the functions of the multilayer, in fact, can be divided on two separate envelopes, an internal bladder and an external structural fabric, which has the main task of resisting the atmospheric agents, while dispersing water and static electricity. This solution is more cost effective and allows a reduction of the fabric weight per square feet, if compared to the multilayer solution which must be employed for the *double-hull*.

There are two main causes of deformation in the exoskeleton design: the buoyancy that acts upwards on the upper surface of the airship envelope, and the weight of the nacelle that acts downwards on the bottom part of the structure. The result is a dilation of the structure along the vertical direction, resulting in deformations greater than one meter. To reduce this effect, the upper and bottom part of ribs and spares are constrained by a set of restraining cables in the vertical-longitudinal plane. Cables are incredibly effective and introduce a negligible mass increasing (about 10kg). The only drawback is that, from the practical point of view, every cable must be sealed to the inner bladder, which must be still able to maintain its helium retention capabilities.

STRUCTURAL ANALYSIS

The loads acting on the structure come from two sources – those resulting from the mass of the structure (including envelopes and landing gear), payload, onboard devices (power unit and avionics) and the forces from the propellers. The propeller actions are simulated as concentrated forces along the rotational axes. Magnitude and direction of these forces are varied over a wide range and differently combined to evaluate the effects of any load configuration. In particular, analysis is performed on the loading combinations which are expected to produce the most severe structural deflections.

The buoyancy calculation is based on the helium volume. Buoyancy is applied in discrete sections across the upper part of the structure in the case of the exoskeleton design and to the septa for the *double-hull* configuration. This approach is clearly not realistic, but it is a fairly good approximation which allows a preliminary analysis without explicitly modelling the interactions between the structure and the helium envelopes. The aerodynamic forces are not considered at this stage of the analysis as they would require modelling a distributed pressure over the whole airship surface. However, they are not supposed to contribute significantly in the structural analysis. These effects could be properly evaluated in the next design phase through a multi-physics analysis, where the fluid-structure interaction and the coupling effects are modelled.

The structural analysis is performed using two software packages: MSC.Patran[7] for the surface pre-processing and MSC.Nastran[8] for the structural calculations. A major problem of this kind of analysis is that the software requires that the model is somehow constrained, in order not to produce singular (non invertible) stiffness matrix. This problem, however, could be easily avoided adopting the *inertia relief* method.

Inertia relief is an advanced option in Nastran, that allows the simulation of an unconstrained structure under linear static conditions. This approach avoids the problem of unrealistic stress concentrations which would arise with conventional constraints. Typical applications of this method are the simulation of aircrafts or satellites. According to the inertia relief hypothesis the structure is unconstrained, and the structural inertia is supposed to resists the loadings in such a way that the entire structure is in a state of equilibrium.

In a simulation using inertia relief, the analyst selects a point in the structure which is used as a "support". The FEA solver then applies a distribution of uniform acceleration such that the induced inertial forces and the design loads (pressure and forces) produce a reaction

force of zero magnitude on the same support, thus resulting in a system of forces in equilibrium.

When the "inertia relief" option is invoked in a static analysis, MSC.Nastran calculates the resultant force in all directions, and thus the field of acceleration that must be applied to the entire structure to reach the equilibrium.

- **Results and Comparison of the Two Models**

The structural design in this project was assisted by a number of structural analyses, which have allowed the calculation of member thicknesses, the geometry and hence the total mass of the proposed structure. These values, combined with information regarding the loads on the structure, were compared with the aerostatic lift generated from the buoyancy of the helium. The objective was to estimate the minimum airship length. It was found that the exoskeleton a minimum length of *32m* is required, while the double-hull length cannot be less than *36m*. Once the minimum required length was calculated, a structural comparison was performed between the two configurations.

- **Displacements**

Both models exhibit displacements that are within acceptable limits of *500mm* for the majority of the load cases. This value was verified on the ETF simulator, changing the propellers positions, to verify that the airship is still able to maintain complete controllability even under the worst deformation scenario. This is the results of several adjustments/iterations on the design of the two configurations. For the exoskeleton model, for example, the first analysis gave excessive deformations, which were reduced through the expedient of the restraining cables, which prevent the structure to open up in the vertical direction, under the action of two contrasting force systems.

As for the *double-hull* model, a similar analysis has been performed, with restraining straps that joined the top and bottom ends of the supporting arms, to observe whether the displacements would still be as important. Results showed that displacements relative were greatly decreased. For the *double-hull* model, the simulation was not entirely realistic since the hulls themselves were not included, thus it was not possible to investigate how the restraining straps interacted with the membrane and the resultant stresses on both bodies.

- **STRESS Analysis**

After the comparison, it was found that the results from the two models were quite similar. The dual-hull design performed particularly well due to its optimal stress distribution, which did not exceed *300 MPa* in any point in the structure. On the contrary the exoskeleton showed a situation of critical stresses during take-off when the structure is completely supported by the ground, but the vertical axis propellers are pulling the airship upwards. Results could be further refined considering the alleviating effect of the buoyancy, which reduces the load by 5% in operational conditions. The buoyancy action, however, is similar on the two configurations, so that it can be stated that the buoyancy introduction cannot change significantly the overall conclusions on the structural comparison. The absence of buoyancy, moreover, is a condition that is actually experienced by the structure during the construction phase, when the structure must be capable of resisting the stress driven by its own weight.

CFD COMPUTATION

Preliminary fluid dynamic analysis[9] has been performed on the two different architectures through a commercial code (STAR-CCM+) that solves the complete set of Navier-Stokes equations on structured/unstructured computational domains, using a finite volume method. Also, this program is able to perform the unsteady analysis, to evaluate the interaction between aerodynamic field and structural vibrations.

The Steady RANS equations have been solved using the sequential algorithm based on the SIMPLE method with a second order discretization model on a Polyedrical mesh.

In order to model the boundary layer phenomena, ten prism layers have been extruded from airship wall with a spacing near wall surface such as not to exceed *30* for the y^+ value.

A realizable k-ε turbulent model with a suitable wall functions model has been used.

Geometrical dimensions of domain, compared to the length of the airship, are large enough to avoid the flow field around the airship to be affected by numerical external condition (Fig. 6).

The software provides, of course, the generation of a grid mesh which is, for both models, a full polyhedral mesh having the following features:

- *double-hull* (Fig. 7) : numbers of cells ~ 3.5E6
- *soap-shaped* (Fig. 8) : numbers of cells ~ 3.0E6

Nautilus invested the early stage of the project in the development of a complete and refined Flight Simulator, which proved to be essential for supporting the whole design process of this non conventional unmanned airship. In particular, the flight simulator provides an effective tool for the design and test of the innovative flight control system and its following integration in the platform on-board computer. Due to the extreme importance of such a tool, the implementation of a flight simulator for the prototype has been considered strategic.

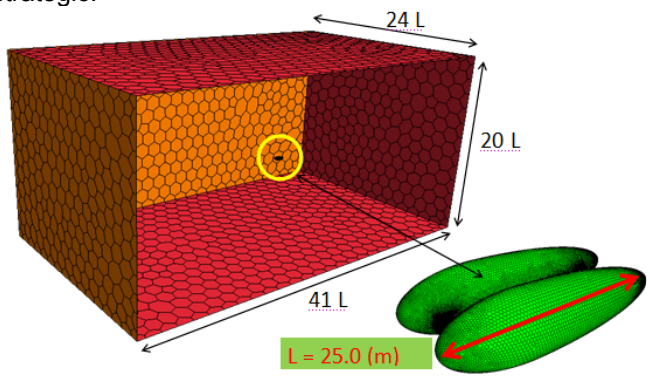

Figure 6 – Computational domain

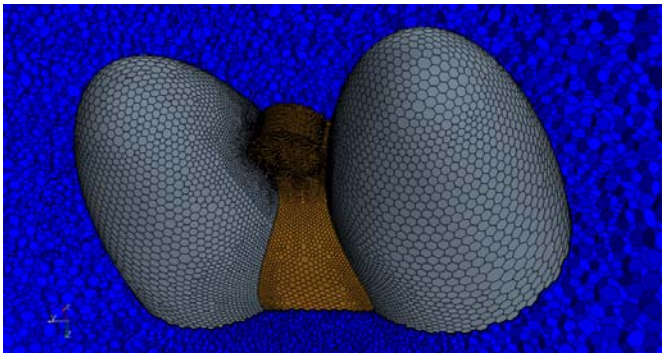

Figure 7 – Double-Hull Mesh

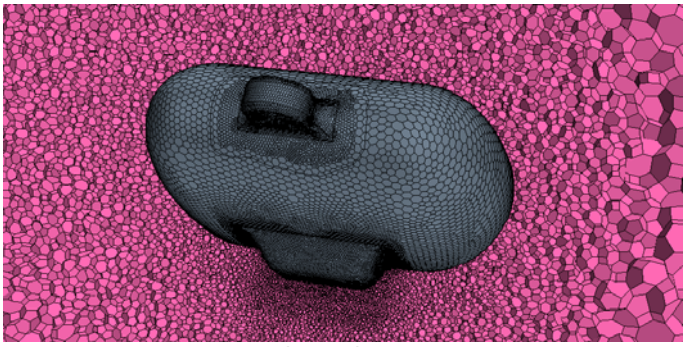

Figure 8 – Soap-Shaped Mesh

Look-up tables currently used on the demonstrator flight simulator are very wide. Several different flight speeds are considered for each of the 6 aerodynamic coefficients, in order to evaluate the influence of Reynolds number. Given two planes of symmetry (x-y and x-z) but keeping nevertheless the possibility for the airship to move in any direction, aerodynamic analysis should be performed on the following ranges: $0° \le \beta \le 180°$ and $0° \le \alpha \le 90°$. A complete aerodynamic analysis thus requires 120 test points for each speed: very low speed (V=2 m/s), speed near to the maximum vertical climbing rate (V=4 m/s), speed near to the maximum wind speed in hovering, maximum rate of descent (V=8 m/s) and speed near to the maximum flight speed (V=20 m/s), according to what is reported in table 1.

Alfa/ Beta	α=0°	α=9°	α=12°	α=15°	α=18°	α=20°	α=29°	α=40°	α=65°	α=90°
β=0°	2,4,8,20	4,8,20	2	2,4,8	4,8		2,4,8	2,4,8	2,4,8	2,4,8
β=9°	4,8,20	4,20		4	4		4	4	4	
β=18°	2,4,8	4,8	2	2,4,8	4,8		2,4,8	2,4,8	2,4,8	
β=27°	4,8	4		4	4		4	4	4	
β=36°	2,4,8	4,8	2	2,4,8	4,8		4,8	4,8	2,4,8	
β=45°	4,8	4		4	4		4	4	4	
β=65°	2,4,8	4,8	2	2,4,8	4,8		4,8	4,8	2,4,8	
β=90°	2,4,8	4	2	2,4	2,4	4	4	4	2,4	
β=115°	4,8	4			4	4	4	4	4	
β=140°	2,4,8	4,8		2	2,4,8	4,8	4,8	4,8	2,4,8	
β=160°	4,8	4			4	4	4	4	4	
β=180°	2,4,8	4,8		2	2,4,8	4,8	4,8	4,8	2,4,8	

Tab.1 – Reference look-up table

The aerodynamic coefficients calculated through the aerodynamic analysis are collected in look-up table form and represent the aerodynamic flight simulator database[11]. Three-dimensional numerical interpolation is performed at each time step for the desired values of flight speed, angle of attack and sideslip angle.

For a preliminary analysis, it has been decided to reduce the number of points to 21 and to just one (low-medium) speed value (V=10 m/s), even if further information for lower Reynolds number would be highly recommended.

In order to reduce computational cost, a Coarse Mesh has been used (Cell Number ~ 3E6). Considering the preliminary state of design development, this has been considered a fairly good compromise between computational costs and numerical accuracy.

In both cases the nacelle takes up a volume of *1/40* of the gas volume. A length of *25m* has been considered for both the solutions, as the minimum prototype dimension estimated through the feasibility analysis. Effective dimension, however, has actually a small importance for the comparison, as results are given in a non-dimensional form.

For the aerodynamic analysis a body reference frame has been adopted: it is based on three orthogonal axes with the origin (O) in the longitudinal plane of symmetry, located centrally along the maximum overall airship length. More precisely:

- the *X* axis lays in the longitudinal plane and is oriented towards the airship prow;
- the *Z* axis is oriented downwards and contained in the longitudinal plane of symmetry.
- the *Y* axis is positive starboard, to form a right-handed reference frame;

Reference conditions for the calculation of the nondimensional forces and torques are reported in Tab.2. Reference dimensions are the maximum dimension along the *Z* axis for torques and the maximum airship width for the Reynolds number.

Test Speed V = 8 [m/s]		
AIR PROPERTIES		
Density = 1,225 [kg/m^3] Viscosity = 1,7894·10^{-5} [kg/m s] Temperature = 288,15 [°K] Pressure = 1013,6 [mbar]		
Shape	Dual-Hull	Soap-Shape
Length L [m]	25	25
Gas Volume Vol [m^3]	1007,20	1356,30
Reference area S= Vol$^{2/3}$ [m^2]	100,48	122,51
Reference length d [m]	6,26	7,21
Characteristic length b [m]	12,50	12,70
Reynolds Number	6,85·10^{-6}	6,96·10^{-6}

Tab.2 – Reference Physical Values

For the preliminary analysis only the configuration of first line/first column of Table 1 have been considered.

Components of the speed vector *V* are calculated according to the scheme of Fig.9:

$$u = V \cos\alpha \cos\beta$$
$$v = V \sin\beta$$
$$w = V \sin\alpha \cos\beta$$

where *u*, *v*, and *w* are, respectively, the linear speed components in the *x*, *y* and *z* body-axis reference frame.

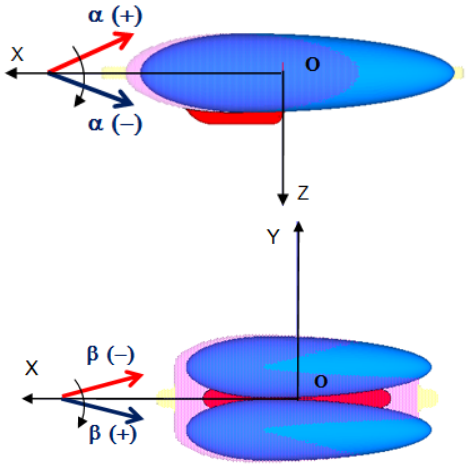

Figure 9 – Reference system and notations

The most interesting results for a comparison between the two solutions, are reported in the following section.

AERODYNAMIC PERFORMANCES

The comparison of aerodynamic coefficients provides information to evaluate aerodynamic performance of the two solutions in the specific flight conditions. Fig.10 shows the trend of the *X*-wind force as a function of the angle-of-attack α (for $\beta = 0°$). In particular for $\alpha = \beta = 0°$ the difference between the two configuration is almost undetectable on the overall scale: a more accurate analysis of the force values, however, reveals that the aerodynamic force along the *X*-wind axis is 20% less for the soap-shape solution (for the same overall length *L*).
For this flight condition ($\alpha = \beta = 0°$), the pressure coefficient contour plot and the iso-surface Cp_{tot}=0 (separated flow) are reported in Figure 11, for the two configurations.
The pressure distribution and the wake structure are very different, especially in the central zone, but this has little influence on the drag.

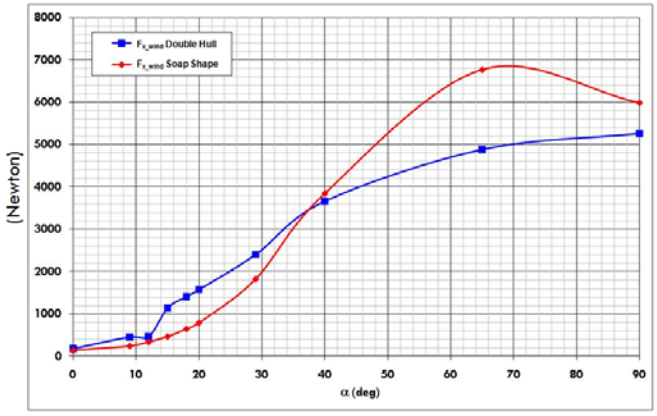

Figure 10 – Xwind force vs angle α

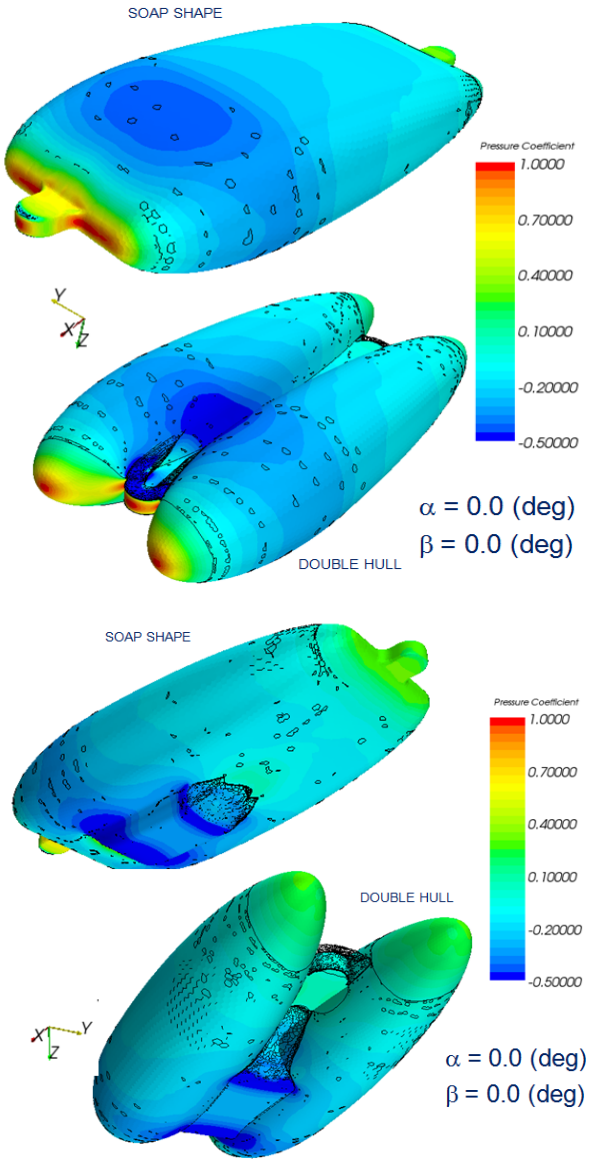

Figure 11 – Countour of Pressure Coefficient & Iso_surface Cp_{tot}=0

The same plot of Fig.10 provide information on the drag action on the two bodies in the situation of vertical descent (α=90 deg): in this case the *Soap Shape* solution has a drag higher of about *12.5%.*
The plot in Fig. 12 shows the force along the *X* wind axis as a function of β for $\alpha = 0°$ and provides information on drag for different values of the sideslip angle. In particular in the situation of cross-wind ($\beta = 90°$), the value of the drag (and therefore of the thrust required to hover) is very different for the two solutions with a pick of about *40%* for the *Double Hull* configuration.
The aerodynamic behaviour of this flight condition is well shown in Fig. 13, where the pressure coefficient contour plot and the iso-surface for Cp_{tot}=0 are reported.
The *Double Hull* configuration shows a high pressure zone larger than the *Soap Shape* and a more extended wake structure. These two circumstances are the main reason of the drag increase.

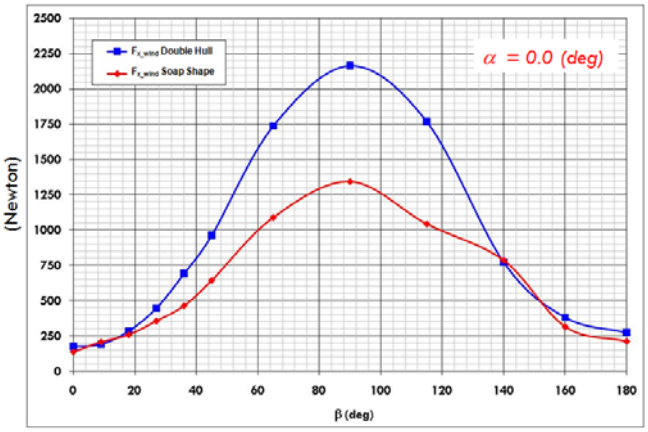

Figure 12 – Xwind Force vs angle β

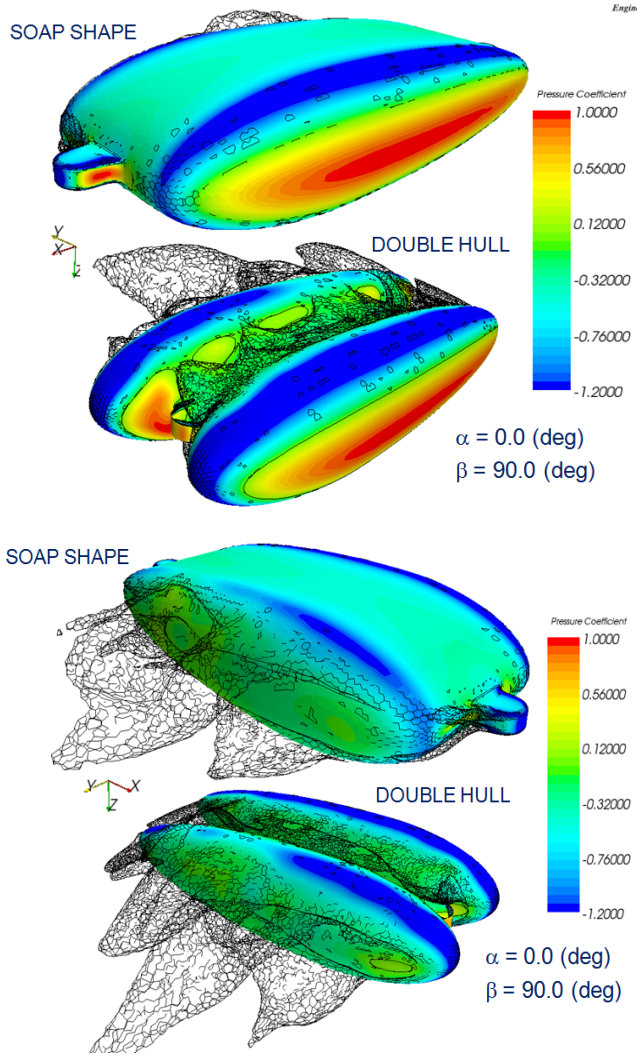

Figure 13 – Countour of Pressure Coefficient & Iso_surface Cp_{tot}=0

Numerical investigation clearly demonstrates that there is a distinct advantage from an aerodynamic point of view for the exoskeleton design, in particular in the "cross-wind" situation (Fig. 13).

STATIC STABILITY

The instable hull behavior in pitching is very well-known; this trend is inverted only for very high values of the angle-of-attack (> 45°). For this reason, a longitudinal Stability Augmentation System (SAS) is strongly recommended, as already shown on the demonstrator[12]. The longitudinal stability coefficient has been compared for the two solutions, as shown in Figure 14: the *Double Hull* configuration presents :

- a not regular trend;
- a lower maximum value;
- a lower slope for very low values of the angle-of-attack (around $\alpha = 0$).

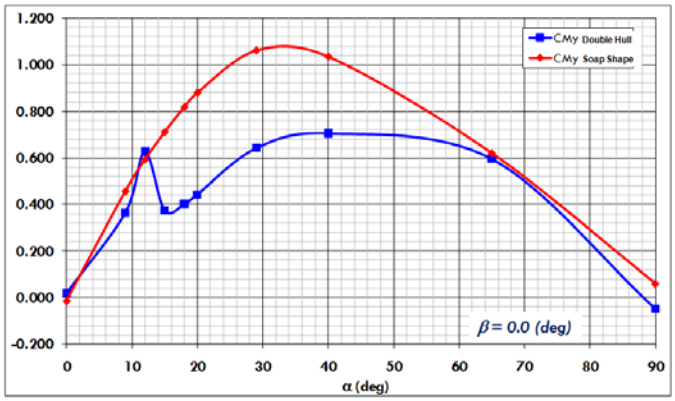

Figure 14 – Pitching moment coefficient; Cm_y vs α

Figure 15 shows the rolling moment coefficient in the cross-wind situation (β = 90°) for small values of the angle-of-attack: the trend reveals static instability also on the lateral-plane and this is the reason why the lateral dynamic behaviour must be augmented by a dedicated SAS. It is interesting to notice, however, that the instability level is almost the same for the two solutions, as shown by the slopes of the two curves.

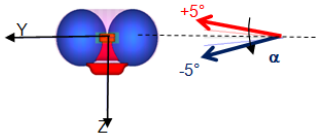

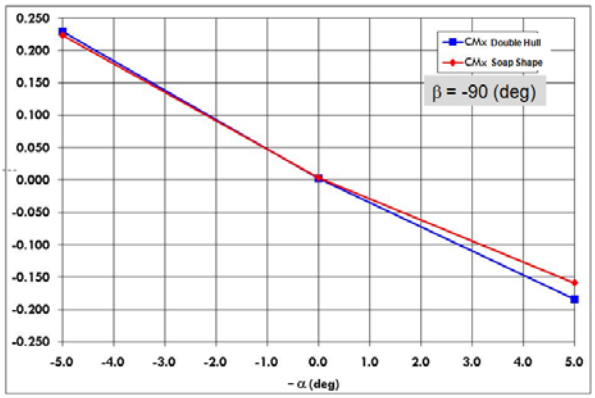

Figure 15 – Rolling-moment coefficient: Cm_x vs α

As far as the directional behaviour is concerned, the situation is highlighted in Fig. 16 where a slightly

favourable condition for the *soap-shaped* solution may be noticed: again, the absolute value shows instability, but the slope of the related curve is lower for the *soap-shaped* configuration.

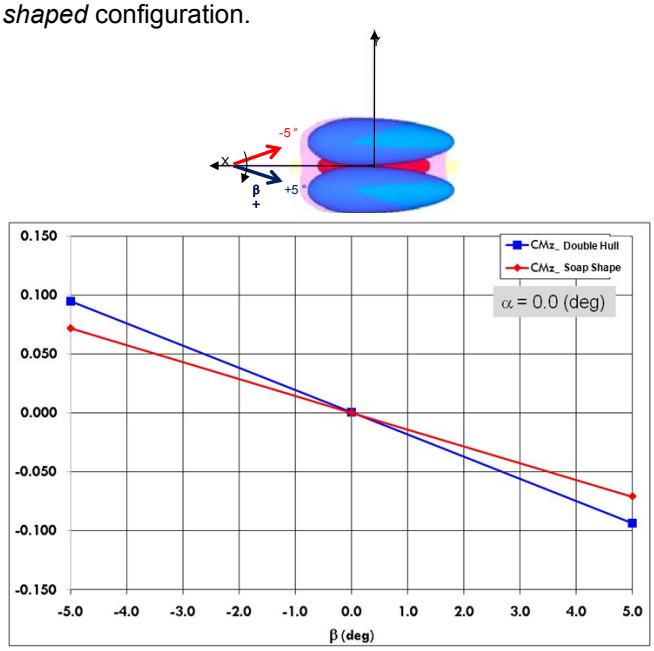

Figure 16 – Yawing-moment coefficient: Cm_z Vs β

From the point of view of the airship stability there are no specific reason which make one configuration prevail over the other.

UNSTEADY ANALYSIS

The aerodynamic/numerical analysis has highlighted remarkable oscillations of the force and torque coefficients in the cross-wind situation for the *Double Hull* configuration. Actually, the β=0° point originates instability phenomena and the analysis of the steady condition presents convergence problems. For this reason, it has been chosen to perform an unsteady analysis and to calculate the aerodynamic coefficients as mean values over a limited time window (Fig. 17). The problem is far less evident for the S*oap Shape* configuration. A further analysis of Fig.13 is useful to explain the phenomena associated to the presence of the two hulls. Apart from the downstream wake, in fact, there is the additional contribution of the flow separation in between the two hulls, which accentuates the vortex strength. The increase in drag shown in Fig.12 is not the only drawback. If the frequency of the aerodynamic oscillation overlaps the structural natural modes, in fact, the phenomenon could degenerate in devastating aero elastic instabilities which could lead to critical structural damages.
The time-histories of Figure 17 have been obtained with a constant forward speed of *8 m/s*: it is possible to observe a coefficient frequency oscillation of about *0.3 Hz*, which corresponds to a Strouhal number of approximately *0.23* (calculated with the characteristic length equal to the maximum airship height - *d=6.26 m*). *St=0.23* is very close to the characteristic value *St=0.18* for which the vortex unsteady separation phenomenon starts to be detectable on sharp-edge obstacles.
Both the static and dynamic analysis, thus, have highlighted that the exoskeleton design is more favourable from the aerodynamic point of view.

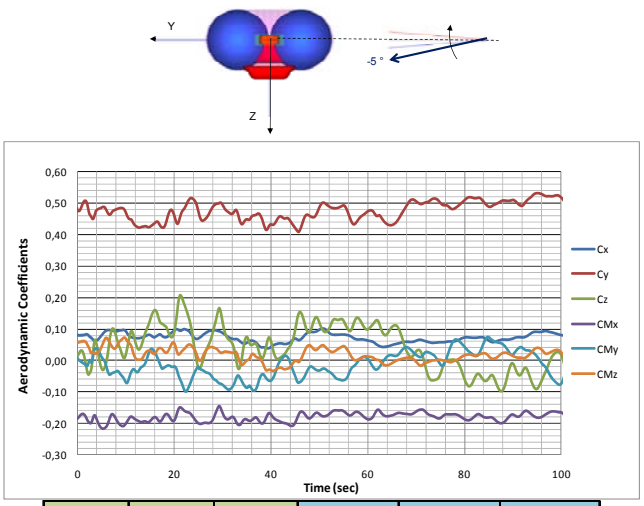

Cx_mean	Cy_mean	Cz_mean	Cmx_mean	Cmy_mean	Cmz_mean
0.0775	0.4785	0.0096	-0.1838	-0.0017	0.0467

Figure 17 – Aerodynamic Coefficients Vs Time
Unsteady simulation - α = -5 (deg) ; β = 90 (deg)

CONCLUSIONS

Numerical analyses revealed that there is a distinct advantage from an aerodynamic point of view for the S*oap Shape* design, in particular in the “cross-wind” situation (hovering with air flow perpendicular to longitudinal symmetrical plane, as shown in Figure 6).

In conclusion, the cost function reveals that the structural and financial advantages of the D*ouble Hull* configurations are roughly balanced by the aerodynamic benefits of the *Soap Shape* design.
In this preliminary analysis important parameters have been omitted from the cost function, because their evaluation has been considered too vague and arbitrary at this stage. The most important parameters, however, have been thoroughly evaluated and have brought to interesting conclusions according to which a third design (Figure 18) is worth being considered. It actually represent a improvement for both the configurations, as it unites the aerodynamic advantages of the *soap-shape* design with the construction benefits of the *Double Hull.*
Figure 18 shows the internal cables and supports used to pull the internal bladder to preserve the soap shape. A robust longitudinal keel has been introduced, as the only rigid structural element, on which all the loads are concentrated, including propulsive, aerodynamic and buoyancy forces. The command and control systems remain unchanged.

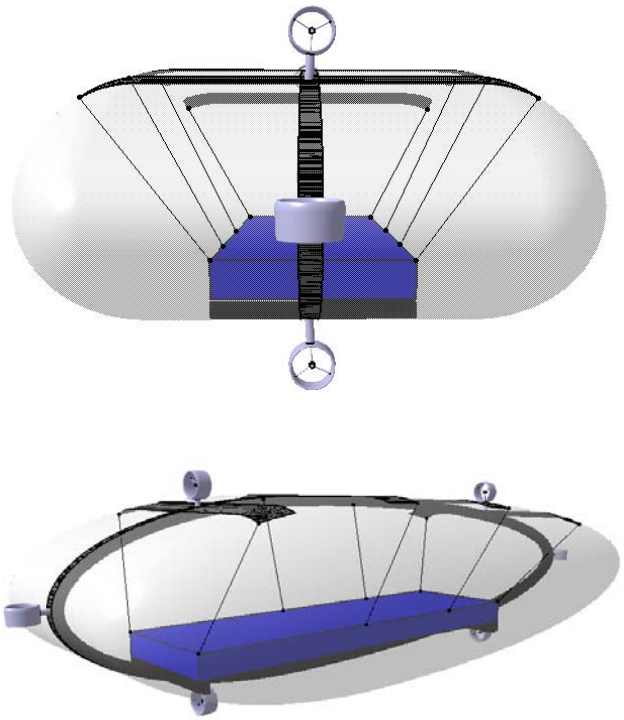

Figure 18 – The new structural solution

ACKNOWLEDGMENTS

The joint academic-private firm research activity presented in the paper has been developed within the ETF06 project supported by Regione Piemonte, Italy.

REFERENCES

[1]Inventors: Gili, P.A., Battipede, M., Icardi, U., Ruotolo, R., Vercesi, P., Owner: Nautilus S.p.A. and Politecnico di Torino, "Dual hull airship controlled by thrust vectoring," N. PCT/EP03/08950, August 2003.

[2]Battipede, M., Lando, M., Gili, P.A., Vercesi, P., "Peculiar Performance of a New Lighter-Than-Air Platform for Monitoring", *Proceedings of the AIAA Aviation Technology , Integration and Operation Forum*, AIAA, Reston, VA, 2004.

[3]Battipede, M., Gili, P.A., Lando, M., "Prototype Assembling of the Nautilus Remotely-Piloted Lighter-Than-Air Platform", *Proceedings of the AIAA Aviation Technology , Integration and Operation Forum*, AIAA, Reston, VA, 2005.

[4]Cappadona, A., Lecca, R., Vazzola, M., Gili, P.A., Farina, P., Surace, C., "Innovative Unmanned Airship Structural Analysis: Dual-Hull and Exoskeletal Configurations", *Proceedings of the 7th International Conference on Modern Practice in Stress and Vibration Analisys*, 8-10 september 2009, New Hall, Cambridge, UK.

[5]Battipede, M., Gili, P., Vazzola, M., "Structure Design for the Elettra Twin Flyers Prototype", *Proceedings of the* 24th Bristol International Unmanned Air Vehicle System Conference, 30th March- 1st April, 2009, Bristol, UK.

[6]CATIA V5R18, Computer Aided Design (CAD) software, Dassault Systems, France.

[7]MSC Nastran 2005, Finite element method (FEM) software MSC Software, USA.

[8]MSC Patran 2005, FEM pre and post-processing software, MSC Software, USA.

[9]STAR-CCM+ User Guide

[10]Visone M., (06/2009), ETF06 Airship Aerodynamic Investigations.

[11]Battipede, M., Gili, P.A., Lando, M., Massotti, L., "Flight Simulator for the Control Law Design of an Innovative Remotely- Piloted Airship", *Proceedings of the AIAA Modeling Simulation and Technologies Conference*, AIAA, Reston, VA, 2004.

[12]M. Battipede, P. Gili, M. Lando, Mathematical Modeling of an Innovative Unmanned Airship for Its Control Law Design, in IFIP International Federation for Information Processing, Volume 202, System, Control Modeling and Optimization, eds.Ceragioli, F., Dontchev, A., Marti, K., Pandolfi, L. (Boston Springer), pp.31-42, 2006.

CONTACT

Piero Gili *:* Aeronautical and Space Department, Politecnico di Torino, ITALY
piero.gili@polito.it

Manuela Battipede : Aeronautical and Space Department, Politecnico di Torino, ITALY
manuela.battipede@polito.it

Matteo Vazzola : Aeronautical and Space Department, Politecnico di Torino, ITALY
matteo.vazzola@polito.it

Michele Visone : Blue Engineering, ITALY
m.visone@blue-group.it

Pierangelo Farina : Blue Engineering, ITALY
p.farina@blue-group.it